Multiple mechanisms contribute to double-strand break repair at rereplication forks in *Drosophila* follicle cells

Jessica L. Alexander[a,b,1], Kelly Beagan[c,1], Terry L. Orr-Weaver[a,b,2], and Mitch McVey[c,2]

[a]Whitehead Institute for Biomedical Research, Cambridge, MA 02142; [b]Department of Biology, Massachusetts Institute of Technology, Cambridge, MA 02142; and [c]Department of Biology, Tufts University, Medford, MA 02155

Contributed by Terry L. Orr-Weaver, October 18, 2016 (sent for review July 30, 2016; reviewed by Johannes Walter and Xiaohua Wu)

Rereplication generates double-strand breaks (DSBs) at sites of fork collisions and causes genomic damage, including repeat instability and chromosomal aberrations. However, the primary mechanism used to repair rereplication DSBs varies across different experimental systems. In *Drosophila* follicle cells, developmentally regulated rereplication is used to amplify six genomic regions, two of which contain genes encoding eggshell proteins. We have exploited this system to test the roles of several DSB repair pathways during rereplication, using fork progression as a readout for DSB repair efficiency. Here we show that a null mutation in the microhomology-mediated end-joining (MMEJ) component, polymerase θ/mutagen-sensitive 308 (*mus308*), exhibits a sporadic thin eggshell phenotype and reduced chorion gene expression. Unlike other thin eggshell mutants, *mus308* displays normal origin firing but reduced fork progression at two regions of rereplication. We also find that MMEJ compensates for loss of nonhomologous end joining to repair rereplication DSBs in a site-specific manner. Conversely, we show that fork progression is enhanced in the absence of both *Drosophila* Rad51 homologs, spindle-A and spindle-B, revealing homologous recombination is active and actually impairs fork movement during follicle cell rereplication. These results demonstrate that several DSB repair pathways are used during rereplication in the follicle cells and their contribution to productive fork progression is influenced by genomic position and repair pathway competition. Furthermore, our findings illustrate that specific rereplication DSB repair pathways can have major effects on cellular physiology, dependent upon genomic context.

oogenesis | break-induced replication | DNA repair | NHEJ | fork collision

Rereplication generates double-strand breaks (DSBs) (1) and can lead to multiple forms of genomic damage commonly observed in human cancers, including DNA fragmentation, chromosome breakage and fusions, repeat expansions, and an increased rate of chromosome missegregation (2–5). Multiple mechanisms of regulation prevent origins from refiring during S phase, but these controls can be overcome experimentally by overexpression of the prereplicative complex component Cdt1 or depletion of its inhibitor Geminin (1). Overexpression of Cdt1 also drives oncogenic transformation in cell culture and is observed in various human cancer cell lines (1). Thus, both the causes of and damage generated by rereplication are observed in human cancers, strongly suggesting rereplication events can be a major driving force in cancer progression.

Although the damage associated with rereplication has been widely observed, the reported mechanism of DSB repair varies. The binding protein, 53BP1, which promotes nonhomologous end joining (NHEJ) and inhibits homologous recombination (HR) (6), forms distinct foci when rereplication is induced in human cells (7). In contrast, the HR protein Rad51 was reported to form foci in rereplicating cells (8, 9) and the HR pathway is required for DSB repair and cell survival after rereplication (10, 11). Microhomology-mediated end joining (MMEJ), an alternative mechanism of end-joining repair that is frequently used in the absence of NHEJ, was also shown to be used for DSB repair during rereplication (6, 11). MMEJ requires limited resection to expose single-stranded DNA ends that anneal at small (1–10 bp) microhomologous sequences (12). DNA polymerase θ (Pol θ) mediates the annealing of microhomologies and subsequent fill-in synthesis required during MMEJ in many organisms (12).

The preferred pathway for DSB repair largely is governed by cell cycle stage (6). Resection-mediated repair, such as HR and MMEJ, is promoted by S-CDK activity and thus is used during S and G2 phases of the cell cycle, consistent with the timing of rereplication events. NHEJ is active throughout the cell cycle, but is preferred during G0/G1 when there is no competition from HR. Pathway choice is ultimately the result of competition between repair proteins for DSB substrates and is influenced by availability and activity of pathway components on their preferred DNA substrates. Studies in budding yeast demonstrated direct competition between HR and NHEJ for DSB repair after rereplication (5), indicating repair pathways may compete for substrates, as has been observed for DSBs generated by other sources of damage.

Here we use the *Drosophila* ovarian follicle cells, which exhibit rereplication under precise developmental control, to define the

Significance

Repeated activation of the same DNA replication origin, termed "rereplication," is one developmental strategy to increase gene copies for high levels of protein production. However, it also generates DNA double-strand breaks and can lead to genome instability. We present evidence for competition between different pathways of double-strand break repair during rereplication in *Drosophila* follicle cells. Loss of DNA polymerase θ (Pol θ), which operates in an error-prone repair mechanism named "microhomology-mediated end joining," impedes the progress of rereplication forks at a specific genomic locus. Pol θ-mediated repair is also used in the absence of classical end joining, but only at certain regions. Our findings suggest that genomic context has a major impact on genomic stability and mutagenesis in rereplicating DNA.

Author contributions: J.L.A., K.B., T.L.O.-W., and M.M. designed research; J.L.A. and K.B. performed research; J.L.A., K.B., T.L.O.-W., and M.M. analyzed data; and J.L.A., K.B., T.L.O.-W., and M.M. wrote the paper.

Reviewers: J.W., Harvard Medical School; and X.W., The Scripps Research Institute.

The authors declare no conflict of interest.

Freely available online through the PNAS open access option.

Data deposition: The aCGH datasets have been deposited in the Gene Expression Omnibus (GEO) database, www.ncbi.nlm.nih.gov/geo [accession nos. GSM432742 and GSM1354444 (wild-type controls), GSE66691 (*lig4*, *spn-A*, and *brca2* mutants), and GSE86012 (all other mutant data reported here)].

[1]J.L.A. and K.B. contributed equally to this work.

[2]To whom correspondence may be addressed. Email: mitch.mcvey@tufts.edu or weaver@wi.mit.edu.

This article contains supporting information online at www.pnas.org/lookup/suppl/doi:10.1073/pnas.1617110113/-/DCSupplemental.

mechanisms of DSB repair required to maintain fork elongation during rereplication. Rereplication occurs at six loci, termed *Drosophila amplicons in follicle cells* (*DAFCs*). The *DAFCs* have specific replication origins that use the same machinery as the canonical S phase (13). Bidirectional fork movement away from the origin produces a gradient of amplified DNA spanning ~100 kb at each *DAFC* (14). One of the defining features of DNA rereplication in follicle cells is the amplification of the eggshell (chorion) protein genes (13). Two chorion gene clusters, located on the *X* and third chromosomes, undergo rereplication to increase gene copy number 16- and 60-fold, respectively (13). Female flies with hypomorphic alleles of genes involved in origin firing exhibit reduced gene amplification, resulting in deficient chorion production and a visible thin eggshell phenotype (13). Gene amplification is therefore a developmental strategy to increase the amount of DNA template available for transcription so that a large amount of protein can be produced in just a few hours.

Precise and coordinated timing of rereplication origin firing at the *DAFCs* makes the follicle cells an ideal system in which to track fork progression. Origin firing at the *DAFCs* begins at a specific developmental stage, 10B, across all follicle cells of a given egg chamber in the absence of genome-wide replication (13). This exact timing of origin firing permits identification of replication forks at defined points after replication initiation, allowing real-time tracking of fork progression. Defined timing of replication initiation also enables fork progression to be compared between different mutants, making it possible to dissect the pathways involved in maintaining fork elongation after rereplication events (15).

We previously found that fork progression at the *DAFCs* is reduced in the DNA ligase 4 (Lig4) null mutant (16), implicating NHEJ for the efficient repair of DSBs at damaged rereplication forks. Here we use this developmental system to evaluate the contribution of Pol θ-mediated MMEJ to DSB repair during rereplication. We find that Pol θ has site-specific effects on rereplication fork progression, suggesting MMEJ is particularly important for rereplication DSB repair in certain genomic contexts. Furthermore, we uncover compensatory repair mechanisms that operate in the absence of individual repair pathways and show evidence for antagonistic effects between NHEJ and HR.

Results

Absence of Pol θ Perturbs Chorion Gene Transcription and Eggshell Formation. Pol θ is important for MMEJ repair of DSBs in many organisms, including *Drosophila*, *Caenorhabditis elegans*, zebrafish, and mice. In *C. elegans*, it is essential for repair of DSBs located at the site of collapsed replication forks (17). Pol θ and other replication-related genes are frequently overexpressed in a number of cancer types and high levels of Pol θ expression strongly correlate to poor patient survival (18). This overexpression may confer an advantage to cancer cells and alleviate replication stress by promoting DSB repair at sites of replication fork collapse. We therefore investigated whether Pol θ, encoded by mutagen-sensitive 308 (*mus308*) in *Drosophila* (12), is involved in DSB repair during rereplication in *Drosophila* follicle cells and whether its loss might impair the production of proteins involved in eggshell development. Indeed, we found that null mutants in *mus308* exhibit a sporadic eggshell defect (Fig. 1 *A*, *iii* and *vii*), indicating MMEJ repair may be required for gene amplification. During the process of chorion deposition, follicle cells leave behind an obvious hexagonal "footprint" (Fig. 1 *A*, *v*) (19). We found that these chorion footprints are diminished in *mus308* mutants (Fig. 1 *A*, *vii*). The *mus308* phenotype differs from other amplification mutants (13), because the defects are variable both between eggs and within individual eggs, resulting in a "patchy" eggshell with uneven chorion deposition that

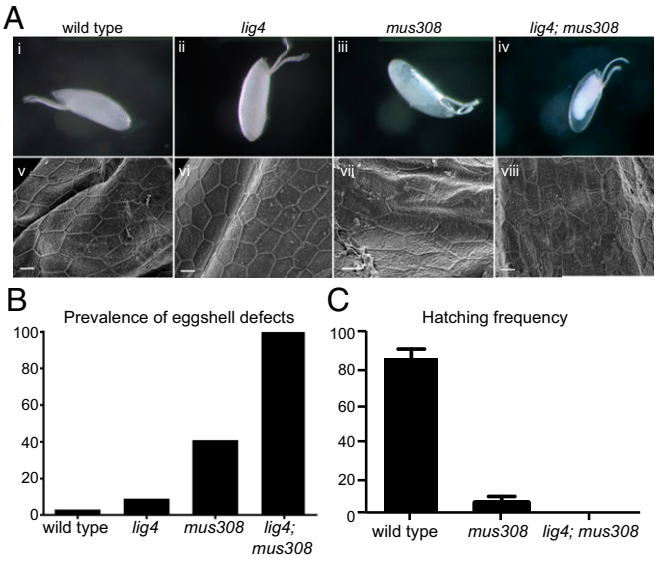

Fig. 1. Eggs laid by *mus308* and *lig4; mus308* females have compromised eggshell integrity. (*A*, *Top*) Light micrographs of eggs laid by (*i*) wild-type w^{1118}, (*ii*) *lig4*, (*iii*) *mus308*, and (*iv*) *lig4; mus308* females. (*Bottom*) Scanning electron micrographs of eggs from (*v*) wild-type w^{1118}, (*vi*) *lig4*, (*vii*) *mus308*, and (*viii*) *lig4; mus308* females. (Scale bars, 10 μm.) (*B*) Prevalence of eggshell defects (percentage of eggs with uneven chorion deposition) in wild-type w^{1118} and mutant backgrounds. $N = 155$ (wild type), 422 (*lig4*), 469 (*mus308*), and 57 (*lig4; mus308*). (*C*) Hatching frequency (percentage of eggs with empty eggshells) for wild-type w^{1118}, *mus308*, and *lig4; mus308* females. Error bars are the SD of three independent trials. A total of 300–500 eggs were scored for each trial of wild-type control and *mus308* and 30–60 eggs for each trial of *lig4; mus308*.

affects 41% of eggs oviposited (Fig. 1 *A*, *iii* and *B*). These eggshells have a glassy appearance within the patches of reduced chorion footprints (Fig. 1 *A*, *iii*). Consistent with the eggshell defects, eggs laid by *mus308* females exhibit only a 4.97% hatching frequency, compared with 85.1% from wild-type females (Fig. 1*C*).

A thin eggshell phenotype is commonly the result of mutations that reduce the number of origin firings at the *DAFCs*, resulting in less DNA template for chorion gene transcription (13). We measured copy number over the *DAFC* origins by quantitative PCR (qPCR) at the final stage of amplification, stage 13. We found that copy number is not significantly reduced at any of the *DAFCs* in *mus308* follicle cells relative to wild type (Fig. S1*A*). Therefore, the *mus308* thin eggshell phenotype is not caused by reduced origin firing at the *DAFCs*.

To determine whether chorion gene transcription is reduced independently of amplification levels, we measured relative mRNA levels by RT-qPCR from stage 13 egg chambers. We found that *mus308* mutants have significantly decreased levels of chorion transcripts at four of the six genes measured, located within both *DAFC-7F* and *DAFC-66D*: *Cp7Fa*, *Cp38*, *Cp16*, and *Cp18* (Fig. 2). Therefore, loss of Pol θ function likely causes a thin eggshell phenotype by reducing mRNA expression of the chorion genes.

Follicle Cell Replication Programs Occur Normally in Pol θ Mutants. During their differentiation, follicle cells go through two cell cycle transitions that are coordinated with the egg chamber developmental stages. The follicle cells proliferate by mitosis during stages 1–6, increase their genome ploidy to 16C via the endocycle in stages 7–9, and finally undergo amplification beginning in stage 10B through the end of follicle cell development in stage 13 (20). To determine whether defects in DNA replication and/or repair before gene amplification could contribute to the unusual *mus308* eggshell phenotype, we examined the

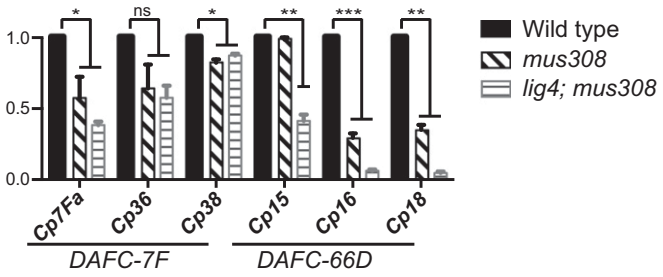

Fig. 2. Pol θ-mediated end joining is required for normal chorion transcript levels. RT-qPCR was performed with cDNA from stage 13 egg chambers. The relative transcript amount (shown on *y* axis) was calculated by first calibrating to the control gene transcript *Rp49*, and then comparing that change to wild-type *mus308/TM6B* siblings. Error bars are the SD of two biological replicates. Significance was measured by Fisher's least significant difference (LSD). **P* < 0.05, ***P* < 0.01, ****P* < 0.001.

replication program across follicle cell development. Accumulation of unrepaired DSBs can lead to checkpoint activation and cell cycle arrest (21). Therefore, we reasoned that DSBs could go unrepaired in the absence of the MMEJ pathway and thus delay cell cycle progression in the follicle cells. To ensure that *mus308* follicle cells complete mitosis at the appropriate stages, we isolated whole ovaries from wild-type and *mus308* females and stained with antibodies against phosphorylated histone H3, a marker of mitosis (22). We found *mus308* mutants undergo mitosis until stage 6, indicating that mitotic cell cycle progression is not affected by loss of Pol θ (Fig. S2*A*). We also measured the relative amount of 2C, 4C, 8C, and 16C follicle cell populations by FACS sorting (Fig. S2*B*). The percentage of nuclei in each peak was comparable between *mus308* and wild type, consistent with *mus308* follicle cells completing three endocycles without cell cycle delays (Fig. S2*B*, *Right*).

To confirm that amplification initiates normally in *mus308* mutants, we labeled follicle cells with the thymidine analog ethynyl deoxyuridine (EdU), which specifically marks the *DAFCs* due to the absence of genome-wide replication after stage 9 (13). EdU labeling confirmed that amplification initiates across all follicle cells at stage 10B in both wild-type and *mus308* egg chambers, consistent with the proper timing of origin firing (Fig. S2*C*). Together, these data demonstrate that cell cycle progression and the developmental onset of gene amplification occur normally in *mus308* follicle cells and that the absence of Pol θ does not perturb follicle cell development.

MMEJ Is Required for Continued Fork Progression During Rereplication in a Site-Specific Manner. We previously found that rereplication at the *DAFCs* generates DSBs, requires the DNA damage response, and the NHEJ repair component Lig4 is necessary for continued fork progression (16). The *mus308* mutant permitted us to evaluate potential contributions of MMEJ to repair of DSBs due to rereplication. We first asked whether DSBs were present in *mus308* mutants by staining EdU-labeled follicle cells with antibodies against the DSB marker γH2Av. Similar to wild type, γH2Av colocalized with EdU beginning in stage 10B in *mus308* follicle cells (Fig. S2*D*), indicating DNA damage is generated and detected by the checkpoint.

To evaluate the role of MMEJ in repair of DSBs at the *DAFCs*, we measured fork progression at the *DAFCs* in *mus308* follicle cells. Unrepaired DSBs within the *DAFCs* will block all subsequent replication forks on the same DNA strand from moving beyond the break site, reducing overall fork progression. We measured fork progression using microarray comparative genomic hybridization (aCGH) paired with half-maximum distance analysis. This analysis uses aCGH to measure copy number across each of the *DAFCs*, followed by calculating the distance between the left and right sides of half-maximum copy number. Reduced fork progression results in a more rapid decrease in copy number and therefore lower half-maximum values (16). Half-maximum analysis was done for five of the six *DAFCs*. *DAFC-22B* is a strain-specific amplicon (14) and thus cannot be compared across all of the mutants analyzed here.

The half-maximum distance was reduced significantly only at *DAFC-66D* and *-7F* in *mus308* follicle cells compared with wild-type *OrR* (Fig. 3*A*). Interestingly, these are the same two *DAFCs* that contain the chorion genes that exhibit reduced transcript levels in *mus308* (Fig. 2). The reduced half-maximum distance at *DAFC-7F* is caused by an asymmetric decrease in the gradient, in which the copy number decreases rapidly within a 20-kb region on the right side of the amplicon (Fig. 3*B*). The site of impeded fork progression is not coincident with the chorion genes, but localizes 10 kb downstream of the most 3′ *DAFC-7F* chorion gene, *Cp38* (Fig. 3*B*). At *DAFC-66D*, copy number is reduced symmetrically on either side of the gradient (Fig. S3), about 5–10 kb from the 5′ and 3′ ends of the chorion genes. Thus, both transcription and

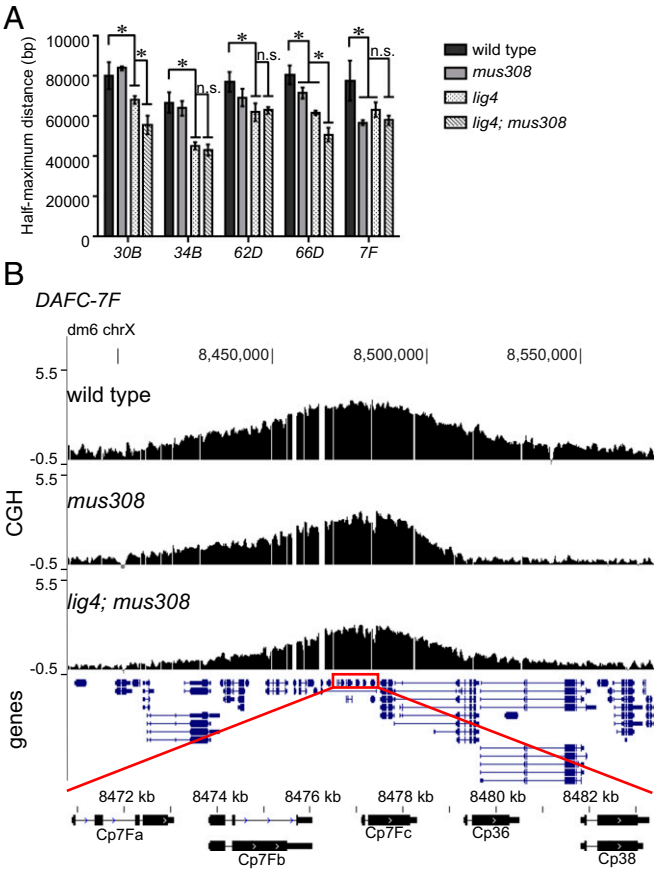

Fig. 3. MMEJ is nonredundant with NHEJ and required for fork progression at *DAFC-7F* and *DAFC-66D*. (*A*) The half-maximum distance was calculated in the wild-type *OrR* and mutant backgrounds for each *DAFC*. Half-maximum distances from *mus308* and *lig4* are compared with wild type and *lig4; mus308* distances are compared with *lig4*. All *lig4; mus308* distances are significantly reduced compared with wild type. The *lig4* half-maximum distances are the same as those previously published (16). Error bars are the SD of three biological replicates. Significance was measured by Fisher's LSD. **P* < 0.05. (*B*) aCGH at *DAFC-7F* in wild-type *OrR* and repair mutants. DNA from stage 13 egg chambers was competitively hybridized with diploid embryonic DNA to microarrays with approximately one probe every 125 bp. Chromosomal position is plotted on the *x* axis; the log2 ratio of stage 13 DNA to embryonic DNA is plotted on the *y* axis. Gene locations are displayed below the CGH data. (*Bottom*) Close-up of the chorion genes.

replication fork progression are reduced at *DAFC-66D* and *-7F* in *mus308* follicle cells, but the effects on fork progression are manifest at distinct positions along the amplification gradients.

The normal half-maximum distances observed at the other *DAFCs* in *mus308* mutants, in contrast to the effects of loss of Lig4 (16), reveal that the MMEJ pathway is not essential for DSB repair during rereplication. It is possible that there is partial redundancy between the NHEJ and MMEJ pathways, with MMEJ serving as a backup and NHEJ being the primary mechanism. We evaluated this by measuring fork progression at the *DAFCs* in a *lig4; mus308* double mutant. The half-maximum distance was reduced significantly compared with the *lig4* single mutant at two sites, *DAFC-30B* and *-66D*, whereas the other three sites were not significantly different from *lig4* (Fig. 3*A*). As expected, all five sites had a reduced half-maximum distance compared with wild type. Thus, MMEJ contributes to repair of DSBs at some but not all of the *DAFCs*.

The single *mus308* and *lig4* mutants did not reduce DNA copy number at any amplicon peak and thus did not affect origin firing (Fig. S3) (16). In contrast, copy number over the aCGH gradient peaks was reduced at all of the *DAFCs* in the *lig4; mus308* double mutant (Fig. S3). This could reflect either a requirement for either Lig4 or Pol θ for origin firing, the ability of stalled forks to inhibit activation of an adjacent origin, or a developmental delay in origin firing. If the latter were true, then the reduced half-maximum distances in *lig4; mus308* could be the result of fork elongation starting at a later time rather than impaired fork progression. We analyzed the timing of origin firing by quantifying copy number at the *DAFC* origins from staged *lig4; mus308* mutant egg chambers. We found that although the total copy number was reduced in *lig4; mus308* mutants, the proper timing of amplification initiation was maintained during egg chamber development (Fig. S1*B*). Therefore, although origin firing is inhibited, the decreased half-maximum distances in *lig4; mus308* reflect impeded fork progression.

Given the reduced copy number of chorion genes in the *lig4; mus308* mutant follicle cells, we examined eggshell morphology and fertility. Whereas eggs lacking *lig4* alone were largely phenotypically normal (Fig. 1 *A*, *ii* and *vi* and *B*), disrupting *lig4* in addition to *mus308* greatly exacerbated the thin-eggshell phenotype (Fig. 1 *A*, *iv* and *viii* and *B*). Eggs laid by *lig4; mus308* females had diminished follicle cell footprints across the egg (Fig. 1 *A*, *viii*), giving these eggs a fully glassy appearance (Fig. 1 *A*, *iv*). These eggshell defects were observed in 100% of the eggs laid by *lig4; mus308* females, consistent with the 0% hatching frequency (Fig. 1 *B* and *C*). We measured relative chorion transcripts by RT-qPCR, and found that in the double mutant the chorion transcripts were significantly decreased at five of the six genes measured (Fig. 2). These results are consistent with the decreased gene copy number at both amplicons (Fig. S1). Together, these results show that absence of both the NHEJ and MMEJ pathways reduces rereplication origin firing, thus reducing transcript levels of the chorion genes and generating uniformly thin eggshells.

Repair by Homologous Recombination Inhibits Follicle Cell Rereplication Fork Progression. We previously found that fork progression is not decreased in spindle-A (*spn-A*)/*rad51* or *brca2* mutant follicle cells (16), leading us to conclude that HR is not used for repair at the *DAFCs*. However, the *Drosophila* genome contains two Rad51 homologs: the ubiquitously expressed *spn-A* (23) and the ovary-specific spindle-B (*spn-B*) (24). To be confident that we were measuring fork progression in the complete absence of Rad51 activity, we performed aCGH and measured the half-maximum distance across each *DAFC* in *spn-A, spn-B* double-mutant follicle cells. In contrast to perturbation of NHEJ or MMEJ, we found the half-maximum distances were increased at all *DAFCs* in the double mutant, although this increase was statistically significant at only three of the five *DAFCs*: *DAFC-30B*, *-66D*, and *-7F* (Fig. 4 and Fig. S3). Additionally, reanalysis of all HR mutant data revealed that the half-maximum distance was also significantly increased in *brca2* follicle cells at *DAFC-30B* and *-66D*, and at *DAFC-66D* in *spn-A* single mutants (Fig. 4). Although disruption of HR affected fork progression, there was no effect on copy number at the origin (Fig. S3). These results demonstrate that HR is active during rereplication in the follicle cells, and its activity is inhibitory to replication fork progression.

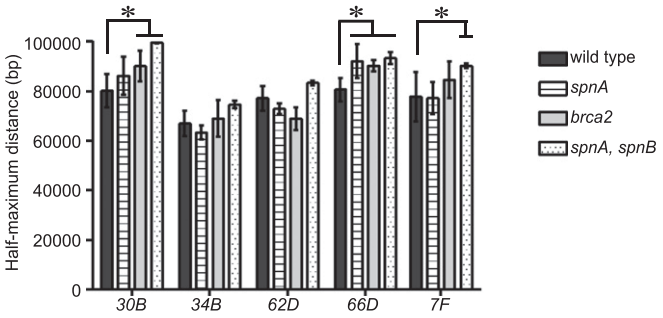

Fig. 4. Loss of HR repair enhances rereplication fork progression. The half-maximum distance was calculated in the wild-type *OrR* and mutant backgrounds for each *DAFC*. The *spn-A* and *brca2* mutant half-maximum distances are the same as those previously published (16). Error bars are the SD of three biological replicates. Significance was measured by Fisher's LSD. $*P < 0.05$.

Fork Progression Is Reduced in Two Break-Induced Replication Mutants. Break-induced replication (BIR) can be used for DSB repair and reestablishment of a replication fork (25), making this pathway an interesting possibility for repair of single-ended DSBs thought to be generated during rereplication (26). To test the role of BIR in repair of rereplication DSBs, we measured fork progression in flies lacking the BIR components Pol32 (27) and Pif1 (28). We observed that the half-maximum distance is significantly reduced at all *DAFCs* in *pol32* and *pif1* mutant follicle cells (Fig. S4). Although these results are consistent with BIR contributing to fork progression at the amplicons, both Pol32 and Pif1 are involved in other aspects of fork progression. Polδ processivity is reduced in the absence of Pol32 (29), and the Pif1 helicase is required for replication through G-quadruplex (G4) secondary structures and hard-to-replicate regions (30). Thus, it remains possible that these other functions account for the measured decrease in fork progression in *pol32* and *pif1* mutants.

Discussion

The *Drosophila* follicle cell amplicons provide a powerful model to delineate the role of distinct repair pathways in the repair of DSBs resulting from rereplication. We find that a unique repair profile exists for each *DAFC* that could be influenced by sequence context, chromosomal location, and developmental timing. Pol θ-mediated MMEJ is required at two positions and it can compensate for NHEJ at some, but not all *DAFCs*. Interestingly, antagonism between HR and NHEJ to repair DSBs also occurs at specific *DAFCs*.

Our results establish that female *Drosophila* lacking the Pol θ homolog exhibit a patchy, thin-eggshell phenotype linked to reduced expression of chorion genes from *DAFC-66D* and *-7F*, but there is no effect on origin firing in the mutant. This apparent effect of Pol θ on transcription may reveal an interesting conflict between replication and transcription in the follicle cells during amplification. Because fork progression is reduced at both *DAFCs*, collapsed forks and unrepaired DSBs likely accumulate 5–10 kb from the chorion genes. Several studies have found that DSB generation leads to a decrease in local transcription, and a recent study in yeast found that a single unrepaired DSB reduces transcription up to 10 kb away on either side of the break site (31). We therefore propose that the absence of MMEJ repair leads to an accumulation of DSBs, inhibiting both fork progression and transcription at certain *DAFCs*.

How Might Various Repair Mechanisms Affect Replication Fork Progression? The fork collision model (2) predicts that collapsed rereplication forks generate single-ended DSBs when a fork meets an unligated Okazaki fragment or overtakes the leading strand of the fork in front of it (26) (Fig. S5*A*). Pol θ has recently been shown to repair collapsed replication forks at secondary-structure-forming sequences in *C. elegans* (17). Thus, Pol θ might also maintain fork progression at the *DAFCs* via microhomology-mediated replication fork restart at a one-ended DSB (Fig. S5*A*). This model is supported by the observation that human bone marrow stromal cells lacking Pol θ are sensitive to camptothecin, which induces one-ended DSBs (32). Such one-ended breaks are also ideal substrates for repair by BIR, which establishes a new replication fork on a homologous template (28) (Fig. S5*A*). However, BIR relies on many components required to establish canonical replication forks (27), making it difficult to study the role of BIR at the *DAFCs* by our current half-maximum analysis. Despite the importance of Pol32 and Pif1 in other aspects of fork progression and repair, the reduced half-maximum distances in these mutants do support the possibility that BIR is important for repair of broken rereplication forks.

Reduced fork progression at the *DAFCs* in *lig4* follicle cells implies two-ended DSBs are also generated during rereplication events (16). It was previously shown that two or more consecutive rounds of rereplication cause DNA fragmentation; although the majority of these fragments were generated from the newly rereplicated DNA, a small proportion was in the template strand (2). Fragmentation of the DNA backbone suggests multiple one-ended DSBs are generated during rereplication, which could be repaired by end-joining mechanisms (Fig. S5*B*). Additionally, removal of extrachromosomal fragments formed during rereplication fork collapse was predicted to generate two-ended DSBs (11) (Fig. S5*C*). Thus, multiple rounds of rereplication at the *DAFCs* may produce numerous two-ended DSBs that could be repaired by NHEJ and MMEJ. It is important to note that DSB repair by end joining is not expected to restore the broken replication fork, but would repair the template strand for continued progression of subsequent forks.

Competition Between Repair Mechanisms During Rereplication. Decreased fork progression in the *mus308* mutant is observed at *DAFC-66D* and within a defined 20-kb region of *DAFC-7F*, revealing these positions are especially dependent on MMEJ repair when the NHEJ pathway is intact. It is possible that the primary sequences at these sites are more favorable for MMEJ repair than the other *DAFCs*. In *C. elegans*, the Pol θ homolog repairs DSBs generated by collapsed replication forks at G4 secondary structures when the G4-unwinding helicase Dog-1 (FancJ) is depleted (17). It is possible that G4 and/or other secondary structures form when extensive single-stranded DNA is generated during rereplication. Thus, specific regions of *DAFC-66D* and *-7F* may contain sequence motifs that are especially sensitive to loss of Pol θ.

The half-maximum distances in the *lig4; mus308* double mutant reveal that MMEJ can compensate for loss of NHEJ at *DAFC-30B* and *-66D*, but not at *DAFC-7F*, *-34B*, or *-62D*. MMEJ is also used for repair after rereplication in human cells, but with reduced efficiency compared with HR (11). This finding is consistent with our observation that MMEJ cannot repair all rereplication DSBs in the follicle cells.

It is interesting that although *DAFC-7F* exhibits reduced fork progression in the absence of either NHEJ or MMEJ, there is no additional effect when both repair pathways are inhibited. However, examination of the aCGH gradients illustrates that loss of these two end-joining pathways influences fork progression at different positions. Whereas fork progression is reduced throughout *DAFC-7F* in *lig4* mutants (16), follicle cells in flies lacking Pol θ exhibit an asymmetric reduction in fork progression within a 20-kb region on the right side of the amplicon. This asymmetry is alleviated in *lig4; mus308* mutants and the gradient resembles that of *lig4* alone. It is interesting to speculate that in wild-type follicle cells, MMEJ competes with NHEJ for repair substrates within this region. In *mus308* follicle cells, competition from MMEJ is removed and thus most DSBs are directed to NHEJ repair. If NHEJ alone cannot efficiently repair DSBs within this region, overall fork progression is decreased. In the absence of both NHEJ and MMEJ, one or more pathways that are not constrained by sequence context may act to repair DSBs in this region.

Increased fork progression in the *spn-A, spn-B* mutant reveals that HR is active during rereplication in the follicle cells and competes with NHEJ for DSB substrates. This competition can be understood in the context of the kinetics of HR, as this pathway likely is too slow for productive DSB repair before the end of follicle cell development. Experiments measuring repair of targeted DSBs estimate HR takes 5–7 h to complete, whereas NHEJ takes 30–70 min (33–35). Amplification in the follicle cells occurs over a 7.5-h developmental window (20). Our aCGH experiments were performed on stage 13 follicle cell DNA, the final stage of development, which lasts for 1 h; this timing places our aCGH measurements 6.5–7.5 h after the first origin firing. Therefore, DSB repair by HR may not be able to promote fork progression within this developmental timescale. This idea is illustrated by the increased half-maximum distances in HR mutants. Absence of HR likely directs more DSBs to the faster NHEJ pathway, thus enhancing overall fork progression.

Alternatively, Rad51-dependent HR might also be used to restart stalled or broken rereplication forks via template switching. The existence of multiple homologous templates might result in recombination intermediates that could impede rereplication fork progression. Multiple rounds of template switching following replication fork collapse have been previously observed in human cells (36, 37). In *Drosophila* follicle cells, loss of Rad51-mediated template switching might also explain the increased fork progression observed in *spn-A, spn-B* mutants.

It is notable that fork progression at *DAFC-34B* and *-62D* is not affected by loss of HR components, nor is there an additional decrease in fork progression in *lig4; mus308* compared with *lig4* alone. It therefore seems that only NHEJ can efficiently repair DSBs to maintain fork movement at these two sites. This dependence on NHEJ may be due to the timing of origin firing. Amplification origins initiate during stages 10B-11 of egg chamber development at *DAFC-7F*, *-30B*, and *-66D* (38). However, *DAFC-34B* and *-62D* undergo another discrete round of origin firing during stage 13 (38, 39) and thus complete fork elongation in only 1 h. Therefore, NHEJ may be the only pathway fast enough to repair DSBs generated from the final origin firing events before the end of follicle cell development.

We also find that the total number of origin firings is reduced in *lig4; mus308* follicle cells across all of the *DAFCs*. Human Pol θ was shown to interact with Orc2 and Orc4 and thus can localize to replication origins (12). It additionally was suggested that Pol θ is important for the temporal regulation of origin firing, although its exact role remains unclear (12). In contrast, our results show that the timing of origin firing is maintained in *lig4; mus308*, albeit reduced, and *mus308* alone has no effect on the level of origin firing during amplification. It is possible that in the absence of both NHEJ and MMEJ, unrepaired DSBs could activate the S-phase checkpoint and thus inhibit origin firing (21). We previously found that null mutations in *chk1* and *chk2* do not increase the number of origin firings at the *DAFCs* (16), contrary to what would be expected if the checkpoint regulates amplification origins. We cannot rule out the possibility, however, that absence of both end-joining repair mechanisms leads to an accumulation of DSBs that may pass some threshold for checkpoint activation and thereby inhibit origin firing.

Measuring fork progression at the *DAFCs* by aCGH is a sensitive and robust tool for the discovery of factors and pathways required for fork progression. Nevertheless, it is limited to pathways with unique genetic components. Deep sequencing of repair junctions

would circumvent these constraints by defining sequence changes diagnostic for each pathway (40). Such a future study will require isolation of purified follicle cells to eliminate contributions from nurse cell DNA undergoing degradation during the stages of egg chamber development in which amplification occurs. This model system will additionally permit future analysis of DNA sequences or chromatin configurations that impact the requirement for distinct repair pathways and that promote fork collision or stalling.

Materials and Methods

Fly Strains. The details of the genotypes and sources of the *Drosophila* strains are presented in *SI Materials and Methods*.

Egg Collection and Scoring. Females were fattened on wet yeast overnight and then placed in a cage with a grape agar plate. The plate was switched every 8–12 h. Eggs were scored for presence or absence of eggshell abnormalities, including missing patches of chorion protein. For imaging, eggs were rinsed twice with PBS, then placed on a glass slide. Images were captured on a Leica MZ16D stereo microscope and a Spot RT3 camera. For hatching frequency, eggs were kept on grape plates at 25 °C for 48 h and then scored as hatched or unhatched.

SEM. For each genotype, 10–20 eggs were collected from grape agar plates. Eggs were prepared for EM as described (19) with modifications noted in *SI Materials and Methods*.

RT-qPCR. Ovaries were dissected from fattened females in PBS. Twenty stage 13 egg chambers were collected for each genotype and stored at −80 °C. Egg chambers were manually homogenized in 300 μL RNA lysis buffer and RNA was isolated using a Zymo Research Quick-RNA Mini Prep kit. cDNA was made using Ambion Retroscript. Copy number was measured by qPCR using *mus308* heterozygous samples as a calibrator and *Rp49* transcript as an expression control.

Nuclear Isolation for FACS. Follicle cell nuclei were isolated as described previously (41) with modifications noted in *SI Materials and Methods*.

Quantitative and Cytological Analysis of Amplification. aCGH, EdU labeling, γH2Av staining, and qPCR were done as described previously (16). Normalization for *mus308* qPCR is described in *SI Materials and Methods*. Phosphohistone H3.3 staining was done as described (42) with modifications noted in *SI Materials and Methods*.

ACKNOWLEDGMENTS. We thank George Bell for bioinformatics support for aCGH and half-maximum analysis; Nikolai Renedo for performing the excision screen that generated the *mus308* null allele; M. Inmaculada Barrasa for bioinformatics support and insight; Nicki Watson and the W.M. Keck Microscopy Facility; Jared Nordman for technical advice; and Jane Kim for helpful discussions. This work was funded by NIH Grants GM57960 and 118098 (to T.L.O.-W.), GM092866 and 105473 (to M.M.), and the MIT School of Science Fellowship in Cancer Research (J.L.A.). T.L.O.-W. is an American Cancer Society Research Professor.

1. Arias EE, Walter JC (2007) Strength in numbers: Preventing rereplication via multiple mechanisms in eukaryotic cells. *Genes Dev* 21(5):497–518.
2. Davidson IF, Li A, Blow JJ (2006) Deregulated replication licensing causes DNA fragmentation consistent with head-to-tail fork collision. *Mol Cell* 24(3):433–443.
3. Finn KJ, Li JJ (2013) Single-stranded annealing induced by re-initiation of replication origins provides a novel and efficient mechanism for generating copy number expansion via non-allelic homologous recombination. *PLoS Genet* 9(1):e1003192.
4. Green BM, Finn KJ, Li JJ (2010) Loss of DNA replication control is a potent inducer of gene amplification. *Science* 329(5994):943–946.
5. Hanlon SL, Li JJ (2015) Re-replication of a centromere induces chromosomal instability and aneuploidy. *PLoS Genet* 11(4):e1005039.
6. Ceccaldi R, Rondinelli B, D'Andrea AD (2016) Repair pathway choices and consequences at the double-strand break. *Trends Cell Biol* 26(1):52–64.
7. Neelsen KJ, et al. (2013) Deregulated origin licensing leads to chromosomal breaks by rereplication of a gapped DNA template. *Genes Dev* 27(23):2537–2542.
8. Melixetian M, et al. (2004) Loss of Geminin induces rereplication in the presence of functional p53. *J Cell Biol* 165(4):473–482.
9. Zhu W, Dutta A (2006) An ATR- and BRCA1-mediated Fanconi anemia pathway is required for activating the G2/M checkpoint and DNA damage repair upon re-replication. *Mol Cell Biol* 26(12):4601–4611.
10. Archambault V, Ikui AE, Drapkin BJ, Cross FR (2005) Disruption of mechanisms that prevent rereplication triggers a DNA damage response. *Mol Cell Biol* 25(15):6707–6721.
11. Truong LN, et al. (2014) Homologous recombination is a primary pathway to repair DNA double-strand breaks generated during DNA rereplication. *J Biol Chem* 289(42):28910–28923.
12. Beagan K, McVey M (2016) Linking DNA polymerase theta structure and function in health and disease. *Cell Mol Life Sci* 73(3):603–615.
13. Claycomb JM, Orr-Weaver TL (2005) Developmental gene amplification: Insights into DNA replication and gene expression. *Trends Genet* 21(3):149–162.
14. Kim JC, et al. (2011) Integrative analysis of gene amplification in Drosophila follicle cells: Parameters of origin activation and repression. *Genes Dev* 25(13):1384–1398.
15. Park EA, Macalpine DM, Orr-Weaver TL (2007) *Drosophila* follicle cell amplicons as models for metazoan DNA replication: A cyclinE mutant exhibits increased replication fork elongation. *Proc Natl Acad Sci USA* 104(43):16739–16746.
16. Alexander JL, Barrasa MI, Orr-Weaver TL (2015) Replication fork progression during re-replication requires the DNA damage checkpoint and double-strand break repair. *Curr Biol* 25(12):1654–1660.
17. Koole W, et al. (2014) A polymerase theta-dependent repair pathway suppresses extensive genomic instability at endogenous G4 DNA sites. *Nat Commun* 5:3216.
18. Wood RD, Doublié S (2016) DNA polymerase θ (POLQ), double-strand break repair, and cancer. *DNA Repair (Amst)* 44:22–32.
19. Turner FR, Mahowald AP (1976) Scanning electron microscopy of Drosophila embryogenesis. 1. The structure of the egg envelopes and the formation of the cellular blastoderm. *Dev Biol* 50(1):95–108.
20. Calvi BR, Lilly MA, Spradling AC (1998) Cell cycle control of chorion gene amplification. *Genes Dev* 12(5):734–744.
21. Ciccia A, Elledge SJ (2010) The DNA damage response: Making it safe to play with knives. *Mol Cell* 40(2):179–204.
22. Hendzel MJ, et al. (1997) Mitosis-specific phosphorylation of histone H3 initiates primarily within pericentromeric heterochromatin during G2 and spreads in an ordered fashion coincident with mitotic chromosome condensation. *Chromosoma* 106(6):348–360.
23. Staeva-Vieira E, Yoo S, Lehmann R (2003) An essential role of DmRad51/SpnA in DNA repair and meiotic checkpoint control. *EMBO J* 22(21):5863–5874.
24. Ghabrial A, Ray RP, Schüpbach T (1998) okra and spindle-B encode components of the RAD52 DNA repair pathway and affect meiosis and patterning in Drosophila oogenesis. *Genes Dev* 12(17):2711–2723.
25. Malkova A, Ivanov EL, Haber JE (1996) Double-strand break repair in the absence of RAD51 in yeast: A possible role for break-induced DNA replication. *Proc Natl Acad Sci USA* 93(14):7131–7136.
26. Abbas T, Keaton MA, Dutta A (2013) Genomic instability in cancer. *Cold Spring Harb Perspect Biol* 5(3):a012914.
27. Lydeard JR, Jain S, Yamaguchi M, Haber JE (2007) Break-induced replication and telomerase-independent telomere maintenance require Pol32. *Nature* 448(7155):820–823.
28. Saini N, et al. (2013) Migrating bubble during break-induced replication drives conservative DNA synthesis. *Nature* 502(7471):389–392.
29. Burgers PM, Gerik KJ (1998) Structure and processivity of two forms of *Saccharomyces cerevisiae* DNA polymerase delta. *J Biol Chem* 273(31):19756–19762.
30. Shimada K, Gasser SM (2012) DNA replication: Pif1 pulls the plug on stalled replication forks. *Curr Biol* 22(10):R404–R405.
31. Manfrini N, et al. (2015) Resection is responsible for loss of transcription around a double-strand break in Saccharomyces cerevisiae. *eLife* 4:4.
32. Yousefzadeh MJ, et al. (2014) Mechanism of suppression of chromosomal instability by DNA polymerase POLQ. *PLoS Genet* 10(10):e1004654.
33. Hicks WM, Yamaguchi M, Haber JE (2011) Real-time analysis of double-strand DNA break repair by homologous recombination. *Proc Natl Acad Sci USA* 108(8):3108–3115.
34. Mao Z, Bozzella M, Seluanov A, Gorbunova V (2008) Comparison of nonhomologous end joining and homologous recombination in human cells. *DNA Repair (Amst)* 7(10):1765–1771.
35. Rapp A, Greulich KO (2004) After double-strand break induction by UV-A, homologous recombination and nonhomologous end joining cooperate at the same DSB if both systems are available. *J Cell Sci* 117(Pt 21):4935–4945.
36. Lee JA, Carvalho CM, Lupski JR (2007) A DNA replication mechanism for generating nonrecurrent rearrangements associated with genomic disorders. *Cell* 131(7):1235–1247.
37. Zhang F, et al. (2009) The DNA replication FoSTeS/MMBIR mechanism can generate genomic, genic and exonic complex rearrangements in humans. *Nat Genet* 41(7):849–853.
38. Claycomb JM, Benasutti M, Bosco G, Fenger DD, Orr-Weaver TL (2004) Gene amplification as a developmental strategy: Isolation of two developmental amplicons in Drosophila. *Dev Cell* 6(1):145–155.
39. Kim JC, Orr-Weaver TL (2011) Analysis of a *Drosophila* amplicon in follicle cells highlights the diversity of metazoan replication origins. *Proc Natl Acad Sci USA* 108(40):16681–16686.
40. Yarosh W, Spradling AC (2014) Incomplete replication generates somatic DNA alterations within Drosophila polytene salivary gland cells. *Genes Dev* 28(16):1840–1855.
41. Lilly MA, Spradling AC (1996) The Drosophila endocycle is controlled by Cyclin E and lacks a checkpoint ensuring S-phase completion. *Genes Dev* 10(19):2514–2526.
42. Schaeffer V, Althauser C, Shcherbata HR, Deng WM, Ruohola-Baker H (2004) Notch-dependent Fizzy-related/Hec1/Cdh1 expression is required for the mitotic-to-endocycle transition in Drosophila follicle cells. *Curr Biol* 14(7):630–636.
43. McVey M, Radut D, Sekelsky JJ (2004) End-joining repair of double-strand breaks in Drosophila melanogaster is largely DNA ligase IV independent. *Genetics* 168(4):2067–2076.
44. Kane DP, Shusterman M, Rong Y, McVey M (2012) Competition between replicative and translesion polymerases during homologous recombination repair in Drosphila. *PloS Genet* 8(4):e1002659.